Electronic Supplementary Material (ESI) for RSC Advances.

Competitive cation binding to Phosphatidylinositol-4,5-bisphosphate domains revealed by X-ray fluorescence

Z. T. Graber,[a†] W. Wang,[b] G. Singh,[c] I. Kuzmenko,[d] D. Vaknin,[b] and E. E. Kooijman[e*]

1 Detailed Methods and Data Analysis

For completeness of this Section, parts of it also appear in the main text.

1.1 Experimental set-up and monolayer details

X-ray reflectivity (XR) and near-total-reflection fluorescence (XNTRF) measurements were conducted on the liquid surface spectrometer (LSS) at beamline 9ID-C, Advanced Photon Source (APS), Argonne National Laboratory. Figure S1 provides a sketch of the experimental setup. The monolayer is formed by drop-wise deposit (at molecular area 85-100 Å^2/molecule) of PIP_2 stock solution onto the aqueous surface of the subphase solutions that is contained in a Langmuir trough and maintained at constant temperature of 20 °C. The Langmuir trough is encapsulated in an enclosure with thin Kapton windows and purged with water-saturated helium gas to minimize background scattering from air and potential X-ray radiation damage to the samples. An oxygen sensor (S101, Qubit System Inc.) in the trough is used to monitor oxygen levels in the enclosure. The monolayer is compressed by a Teflon barrier to a desired surface pressure of 30 ± 2 mN/m. Surface pressure is monitored by a microbalance made of a Wilhelmy microbalance and filter paper plate. The X-ray measurements are started after the oxygen-helium exchange reaches equilibrium, where the oxygen content inside the enclosure is reduced by a factor of at least 100 with respect to that of the ambient atmosphere. The monolayer is maintained at $\pi \approx 30$ mN/m during the course of the experiments. Radiation damage is monitored by systematically translating the trough laterally to probe fresh surfaces and examine measurement reproducibility. All reflectivity measurements were found to be reproducible.

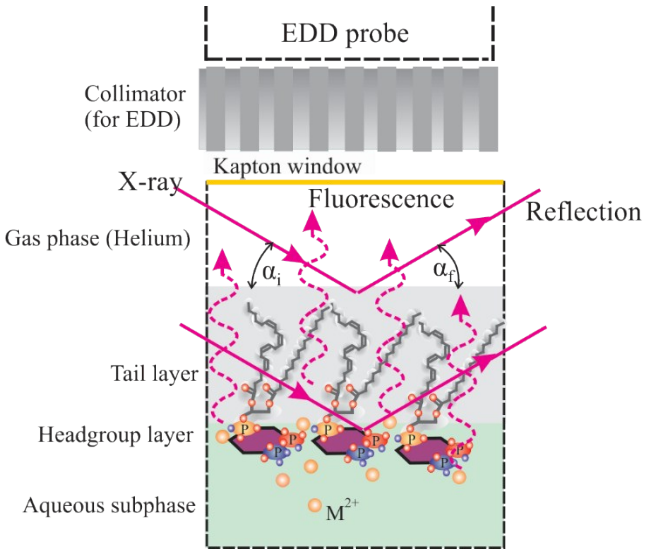

Figure S1: Setup. Illustration of the X-ray fluorescence and reflectivity setup for the PIP_2 monolayer over a subphase containing divalent ions M^{2+}, where M represents Ca or Mg. The box enclosed by the dashed lines is a side view of the interfaces of a vapor phase (water-saturated helium), monolayer and aqueous bulk. The X-ray beam impinges on the surface at an incident angle α_i and reflects at an exit angle α_f and $\alpha_i = \alpha_f$ in a specular reflectivity mode. The probe of the EDD subtends the center of the sample surface with a collimator in front of it to define the EDD footprint that is smaller than the X-ray beam footprint and only accepts

X-ray photons of the fluorescence signals and background scattering (emanated from bulk water and helium) restricted to the surface normal direction with 1 degree acceptance angle.

1.2 X-ray experiments

The highly monochromated and collimated X-ray beam (E = 8.0 keV; wavelength λ = 1.5497 Å) passes through an ionization chamber (to monitor incident beam intensity) and variable beam attenuator (multilayers of nickel foil, for attenuation of the primary incident beam), and is steered onto the aqueous surface by a second monochromator to a desired incident angle α_i with respect to the surface. The specular reflection is collected by a Bicron scintillation detector at an X-ray exit angle $\alpha_i = \alpha_f$. The angular-dependence of both XRR and XNTRF are expressed as functions of Q_z, the z-component (surface normal) of the scattering (wave vector transfer) vector Q. Q_z is related to the incident angle α_i via $Q_z = (4\pi/\lambda) \sin\alpha_i$, and Q_c represents the Q_z that corresponds to the critical angle for total reflection, α_c (= 0.154° at E = 8keV).

The fluorescence signals are collected at a series of α_i near the critical angle α_c by a Vortex energy dispersive detector (EDD, silicon-drift, Vortex-90EX) with a collimator in the front end of the EDD probe, which accepts the X-ray fluorescence of emitted photons in the direction along the surface normal at ~ 1° angular resolution.

Fluorescence signals from pure water subphase are measured as background to be subtracted from those of the relevant samples. The EDD spectra also contain the primary beam signals at E = 8.0 keV mainly from Thomson elastic scattering of bulk water and Compton inelastic scattering (from bulk water and water-saturated helium, at a lower energy shifted from E= 8.0 keV by ≤ 0.1 keV). Both fluorescence and reflectivity data are normalized to incident beam intensity (more details can be found elsewhere [1, 2]).

1.3 X-ray reflectivity data analysis

X-ray reflectivity data, $R(Q_z)$, are normalized to the calculated Fresnel reflectivity (R_F), for an ideally smooth, flat air-water interface [3, 4]. The R/R_F data for a surface monolayer on an aqueous surface can be accounted for in terms of a simplistic, *two-box* (i.e., two-layer) structural model, where one *box* contains the hydrophilic head group, and the other contains the hydrocarbon tail [1, 3, 5]. Each *box* is characterized by a uniform electron density (ρ) and vertical height (l) relative to the interface. Given (ρ_H, l_H) and (ρ_T,l_T), in which subscripts "H" and "T" represent the headgroup and the hydrocarbon tail respectively, a step-like, discrete ED profile across the interfaces, $\rho_0(z)$, is constructed and its corresponding reflectivity $R_0(Q_z)$ is calculated by the Parratt recursion method [1, 3]. The realistic ED profile, $\rho(z)$ is obtained by smearing $\rho_0(z)$ with an interfacial roughness, σ, mainly arising from capillary waves [4], which lowers the $R_0(Q_z)$ by a "Debye-Waller-like" factor, $\exp(-Q^2_z \sigma^2)$ as follows: [1, 3, 4]

$$R/R_F = \left(R_0/R_F\right) e^{-Q_z^2 \sigma^2} \qquad \text{(S1)}$$

The structural refinements are carried out through a least squares optimization method [1].

1.3.1 Calculation of molecular area from reflectivity data

The molecular area, A_{mol}, of PIP_2 can be calculated from these reflectivity data by assuming that a PIP_2 molecule has an acyl-chain length corresponding to the stearic acid tail at the sn-1 position of natural PIP_2. The maximum acyl chain length of stearic acid, l_{Tmax}, can be estimated as ~ 22 Å since each carbon (17 in stearic acid, excluding the carbonyl) contributes ~1.27 Å [6, 7]. The molecular area of the lipid A_{mol}, can be determined based on this maximum (l_{Tmax})and the actual acyl-chain length, l_T, using $2A_0 l_{Tmax} / l_T$, where A_0 is the minimum area available to a single, untilted alkyl chain (~20 Å^2, according to measurements with arachidic acid) [6, 7]. Here we assume that the arachidonoyl chain of natural PIP_2 contributes an equal area, as the stearic acid chain, to the overall area of each PIP_2. Although the organization of arachidonoyl chains is largely unknown, this is a reasonable assumption and leads to a lower bound of the molecular area of PIP_2 (A_{mol} in Table S1). These values are consistent with those obtained from isotherms (A_{mol2}).

1.3.2 Calculation of # of divalent cations bound to PIP_2

The reflectivity data allows for an estimation of the number of divalent cations (M^{2+}) bound to the headgroup of PIP_2, based on a space-filling model[1, 8, 9]. The model assumes the headgroup volume is the sum of volumes of the K^+ ions, M^{2+} ions, water molecules, and the PIP_2 head group. The conservation of electron numbers and constrains on the total volume contained in the two *boxes* (one associated with the acyl chains and the other, more complex, includes the headgroup, water molecules and ions) can be expressed as follows

$$A_{mol} I_H = V_{H,dry} + n_{H2O} V_{H2O} + n_{K+} V_{K+} + n_{M2+} V_{M2+}, \quad \text{(S2)}$$

$$A_{mol} \rho_H I_H = N^e_{H,dry} + N^e_{H2O} n_{H2O} + N^e_{K+} n_{K+} + n_{M2+} N^e_{M2+}, \quad \text{(S3)}$$

Assuming the number of bound K^+ per PIP_2 is unchanged prior to and after M^{2+} binding, we obtain the n_{M2+}, the number of M^{2+} per PIP_2 molecule (see Table 1 and 2 in the main manuscript)[9]. These binding numbers serve as lower limits of actual binding number of Ca^{2+} and Mg^{2+} per PIP_2. In this case we also assume that the divalent ions are dehydrated when they bind to PIP_2, however, Slochower et al. suggested that Mg^{2+} may remain hydrated when it binds to PIP_2[10]. If we assume that a hydration shell of six molecules remains around Mg^{2+}, this reduces the calculated number of bound Mg^{2+} ions to ~0.6 ions/PIP_2.

1.4 X-ray fluorescence data analysis

Surface fluorescence studies have been performed in the past [11, 12] and analytic routines to quantify the surface enrichment of ions have been established [8, 9] and are briefly discussed below. At $\alpha_i < \alpha_c$, the X-rays penetrate into the liquid by a very shallow depth (< 10 nm) in the direction of the surface normal [1, 3]. At $\alpha_i > \alpha_c$, the X-rays penetrate into the bulk by a few micrometers (within the X-ray energy of 8-16 keV typically used for liquid surface scattering). The combination of shallow X-ray penetration depth and surface intensity enhancement arising from evanescence when $\alpha_i < \alpha_c$ provides the surface sensitivity of the XNTRF method. In this study, the fluorescence measurements were conducted over the range $0.5\alpha_c < \alpha_i < 1.5\alpha_c$, corresponding to Q_z = 0.01-0.035Å^{-1}, with a spacing of 0.001Å^{-1} between consecutive Q_z points. The fluorescence data collected at $Q_z < Q_c$ and $Q_z > Q_c$ are referred to as surface fluorescence and bulk fluorescence signal, respectively.

To calibrate the spectral intensity to known quantities of fluorescing ions, we compare fluorescence data from two bulk solutions of $CaCl_2$ (pre-acidified with a small amount of HCl to prevent potential formation and precipitation of $Ca(OH)_2$ at this high $CaCl_2$ concentration) and KCl both prepared at 100 mM with a bare air/water interface. Figure S2 shows the individual bulk fluorescence spectra for Ca^{2+} and K^+. Each spectrum within the energy range shown in Figure S2 is characterized by two emission lines, K_α and K_β, each of which is further profile-fit with a Gaussian-like function centered on the emission line energy. The finite spread of the emission lines is a measure of the EDD energy resolution at each emission line. The bulk fluorescence spectra shown in Figure S2 provide the "standard spectral profile" for each element, which characterizes (1) the relative intensity ratio of K_α to K_β and (2) the relative line(s) intensity ratio of Ca^{2+} to K^+, given the same bulk concentrations. As 100 mM KCl is present in the relevant samples and the K^+ K_β line partially overlaps with the Ca^{2+} K_α line, the standard spectral profiles serve to discriminate the K^+ and Ca^{2+} contribution when both are present in the spectra.

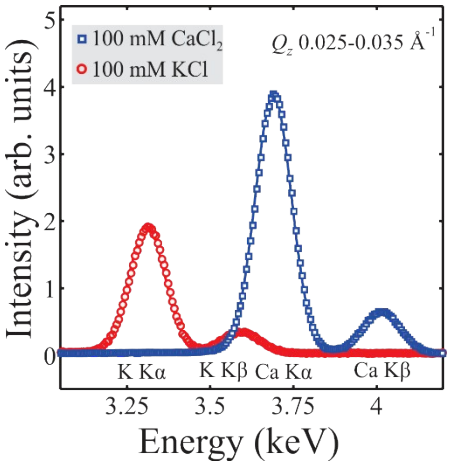

Figure S2: Bulk Fluorescence Spectra. The bulk fluorescence spectra for a pure KCl and a $CaCl_2$ solution as indicated. Both solutions were prepared at 100 mM. $CaCl_2$ solutions were acidified to prevent Ca^{2+} precipitation as $Ca(OH)_2$ (due to the high concentration of $CaCl_2$). The spectra were integrated over Q_z = 0.025-0.035 A^{-1} to demonstrate the relative intensity of emission lines of Ca^{2+} relative to K^+ detected by the EDD.

The Mg^{2+} ion emission lines are K_α = 1.25 keV and K_β = 1.07 keV. These low energy emission lines are outside the sensitivity range of the EDD. At each Q_z, the fluorescence intensity of a specific emission line is integrated over its spread in the spectrum and expressed as a function of sin α_i (i.e., proportional to Q_z). For a solution of fluorescing ions with a bare surface the fluorescence intensity, $I_b(\alpha_i)$, is proportional to its bulk concentration n_b and the volume illuminated by X-ray, and can be expressed as follows:

$$I_b(\alpha_i) = C\left|t_F(\alpha_i)\right|^2 D(\alpha_i) n_b \qquad \text{(S4)}$$

where C is an element-specific scale factor that accounts for elemental fluorescence yield and detector efficiency, $t_F(\alpha_i)$ is the X-ray Fresnel transmission coefficient at a sharp, flat vapor/liquid interface, $D(\alpha_i)$ is the X-ray penetration depth normal to the surface, and n_b is the bulk concentration of the ion [1, 3]. For a thin layer of surface excess ions, their fluorescence contribution, $I_s(\alpha_i)$, can be expressed as follows:

$$I_s(\alpha_i) = C\left|t_F(\alpha_i)\right|^2 n_s e^{-\left|z_{ion}\right|/D(\alpha_i)} \qquad \text{(S5)}$$

where z_{ion} is the z-coordinate of the ion-enriched layer with z = 0 at the monolayer/vapor interface.

For a solution with relatively low cation concentration (< 0.01M) with a bare surface (i.e., no monolayer), the fluorescence comes almost exclusively from the bulk (see the black data points in Figure S3). In this case the ions are randomly distributed throughout the solution, and the very few ions that are observed in the 5 nm surface region are practically beyond the detection limit of the EDD. Thus, for the situation where $Q_z < Q_c$ there is very little to almost no fluorescence signal. For $Q_z > Q_c$, the ions in the bulk solution are excited and we observe detectable fluorescence intensity. For a cation enriched surface bound to PIP_2, the fluorescence signal is observed both below and above Q_c (see Figure S3 in red –signal containing both the surface and bulk contribution). The surface density of cations for a surface covered with a PIP_2 monolayer is given by:

$$n_s = \frac{I_s(\alpha_i)}{I_b(\alpha_i)} D(\alpha_i) n_b e^{z_{ion}/D(\alpha_i)} \qquad \text{(S6)}$$

For known mean molecular area of the lipids, the number of ions per lipid can be calculated by simply multiplying the ion density by the area per lipid. This molecular area is obtained from the isotherms recorded during the preparation of the PIP_2 monolayer. Briefly, PIP_2 was spread at a molecular area between 85-100 $Å^2$/molecule (i.e. at negligible surface pressure) on each of the subphases examined and compressed to a pressure of 30±2 mN/m, monitored by a Whilhelmy balance. The molecular areas obtained from the isotherms are the same (within experimental error) to those extracted from the analysis of the X-ray reflectivity data, see tables S1 and S2 below.

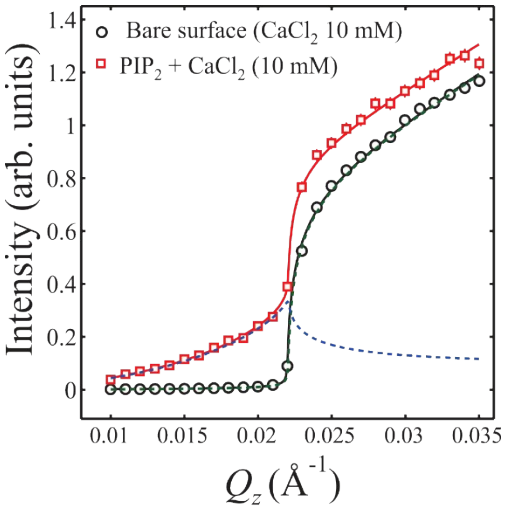

Figure S3: Fluorescence Q_z Dependence. Fluorescence intensities of Ca^{2+} emission line(s) as a function of Q_z for a solution of $CaCl_2$ at concentration of 10 mM covered with a PIP_2 monolayer (red) and an equivalent 10 mM $CaCl_2$ solution with a bare surface (black). Each data point represents the intensity integrated exclusively over the Ca K_α emission line in the spectrum. The solid lines are best-fit profiles calculated in terms of Eqn. 3 for the bulk contribution and the sum of Eqn. 3 and Eqn. 4 for the solution covered with the PIP_2 monolayer. The dashed line is solely due to the surface contribution as expressed in Eqn. 3.

References

1. D. Vaknin, in *Characterization of Materials*, ed. E. N. Kaufmann, John Wiley & Sons, New York, 2012, vol. 2, pp. 1393-1423.
2. W. J. Wang, N. S. Murthy, I. Kuzmenko, N. A. Anderson and D. Vaknin, *Langmuir*, 2013, **29**, 11420-11430.
3. J. Als-Nielsen and D. McMorrow, *Elements of modern X-ray physics*, Wiley, Hoboken, 2nd edn., 2011.
4. P. S. Pershan and M. L. Schlossman, *Liquid Surfaces and Interfaces: Synchrotron X-ray methods*, Cambridge University Press, New York, 2012.
5. K. Kjaer, *Physica B*, 1994, **198**, 100-109.
6. D. M. Small, in *Handbook of Lipid Research*, Plenum Press, New York and London, 1986, vol. 4, ch. 3.
7. K. Kjaer, J. Alsnielsen, C. A. Helm, P. Tippmankrayer and H. Mohwald, *J Phys Chem-Us*, 1989, **93**, 3200-3206.
8. W. Bu, K. Flores, J. Pleasants and D. Vaknin, *Langmuir*, 2009, **25**, 1068-1073.
9. W. Wang, N. A. Anderson, A. Travesset and D. Vaknin, *J Phys Chem B*, 2012, **116**, 7213-7220.
10. D. R. Slochower, P. J. Huwe, R. Radhakrishnan and P. A. Janmey, *J Phys Chem B*, 2013, **117**, 8322-8329.
11. J. Daillant, L. Bosio, J. J. Benattar and C. Blot, *Langmuir*, 1991, **7**, 611-614.
12. W. B. Yun and J. M. Bloch, *Journal of Applied Physics*, 1990, **68**, 1421-1428.